Bone. Author manuscript; available in PMC: 2014 Nov 1.
Published in final edited form as: Bone. 2013 Aug 14;57(1):164–173. doi: 10.1016/j.bone.2013.08.002

Acute Exposure to High Dose γ-Radiation Results in Transient Activation of Bone Lining Cells

Russell T Turner [a,b], Urszula T Iwaniec [a,b], Carmen P Wong [a], Laurence B Lindenmaier [a], Lindsay A Wagner [a], Adam J Branscum [c], Scott A Menn [d], James Taylor [e], Ye Zhang [e,f], Honglu Wu [e], Jean D Sibonga [e]

Author information Article notes Copyright and License information

PMCID: PMC4042434 NIHMSID: NIHMS521003 PMID: 23954507

Abstract

The present studies investigated the cellular mechanisms for the detrimental effects of high dose whole body γ-irradiation on bone. In addition, radioadaptation and bone marrow transplantation were assessed as interventions to mitigate the skeletal complications of irradiation. Increased trabecular thickness and separation and reduced fractional cancellous bone volume, connectivity density, and trabecular number were detected in proximal tibia and lumbar vertebra 14 days following γ-irradiation with 6 Gy. To establish the cellular mechanism for the architectural changes, vertebrae were analyzed by histomorphometry 1, 3, and 14 days following irradiation. Marrow cell density decreased within 1 day (67% reduction, $p<0.0001$), reached a minimum value after 3 days (86% reduction, $p<0.0001$), and partially rebounded by 14 days (30% reduction, $p=0.0025$) following irradiation. In contrast, osteoblast-lined bone perimeter was increased by 290% (1 day, $p=0.04$), 1230% (3 days, $p<0.0001$), and 530% (14 days, $p=0.003$),

respectively. There was a strong association between radiation-induced marrow cell death and activation of bone lining cells to express the osteoblast phenotype (Pearson correlation −0.85, $p<0.0001$). An increase ($p=0.004$) in osteoclast-lined bone perimeter was also detected with irradiation. A priming dose of γ-radiation (0.5 mGy), previously shown to reduce mortality, had minimal effect on the cellular responses to radiation and did not prevent detrimental changes in bone architecture. Bone marrow transplantation normalized marrow cell density, bone turnover, and most indices of bone architecture following irradiation. In summary, radiation-induced death of marrow cells is associated with 1) a transient increase in bone formation due, at least in part, to activation of bone lining cells, and 2) an increase in bone resorption due to increased osteoclast perimeter. Bone marrow transplantation is effective in mitigating the detrimental effects of acute exposure to high dose whole body γ-radiation on bone turnover.

Keywords: murine, bone histomorphometry, osteoblasts, osteoclasts, osteoporosis, bone marrow

1. Introduction

Human exposure to high levels of ionizing radiation can occur as a result of treatment modalities or accident. Also, high dose whole body radiation is a common strategy in biomedical research to ablate bone marrow cells as a prelude to stem cell transplantation. As a side effect, radiation therapy to treat cancer in humans or in biomedical research results in collateral damage to other tissues, including the skeleton [1]. The spectrum of skeletal abnormalities associated with radiation therapy in humans ranges from growth suppression in children to osteopenia, sclerosis, necrosis and sarcomatous transformation at all ages [2, 3]. High dose ionizing radiation is also a risk factor for the development of fractures that typically have prolonged healing times and a high nonunion rate [4]. In spite of compelling human evidence for impaired skeletal function following high-dose ionizing radiation, this complication is rarely considered in bone marrow transplantation studies performed in animal models.

Whole body exposure to high dose ionizing radiation, although uncommon in humans, can occur as a result of nuclear accident [5]. Future manned space travel beyond the earth's protective magnetic field will undoubtedly also increase the potential for exposure to high levels of ionizing radiation, which include particles (electrons, neutrons, protons and atomic nuclei) as well as photons (x-rays and γ-rays) [6]. Importantly, the precise biological effects of ionizing radiation depend upon numerous factors, including species, age, type of radiation, dose and dose rate [5, 7].

Short-duration exposure to more than 1 gray (Gy) of radiation can lead to acute radiation syndrome and in humans > 6 Gy is often lethal. Acute radiation syndrome consists of hematopoietic, gastrointestinal and neurovascular manifestations, the timing and magnitude of which are dose-dependent [8]. The long-term skeletal consequences of surviving acute radiation syndrome in humans have received little attention. However, modeling acute radiation syndrome in animals has demonstrated detrimental effects on bone mass and architecture [9-11].

There has been significant interest in mitigating the detrimental effects of radiation to reduce morbidity and mortality following exposure. Exposure to small (priming) doses of ionizing radiation has been shown to induce cellular radioprotective mechanisms following γ-irradiation [12]. Induction of radioadaptation by this method reduces mortality following subsequent exposure to much higher (challenging) doses of radiation. The state of acquired radioresistance is associated with reduced radiosensitivity and hypercompensation by hematopoietic cells to radiation-induced damage [13]. Although effective in reducing mortality, which may be of particular value for marrow transplantation studies in immune compromised radiosensitive mice, it is uncertain whether low dose radiation-induced radioresistance will impact bone marrow ablation or protect the skeleton from the detrimental effects of high dose irradiation.

Medical intervention in humans, including administration of growth factors (e.g., granulocyte colony-stimulating factor and granulocyte-macrophage colony-stimulating factor to improve immune function, can reduce mortality in individuals accidently exposed to whole body ionizing radiation [14]. Mitigation of lethal intestinal injury, following high local doses of irradiation in mice, has been achieved by intravenous transplantation of bone marrow-derived stromal and hematopoietic stem cells [15-17]. However, it is not clear whether interventions involving growth factor administration or bone marrow transplantation impact the long-duration adverse skeletal effects of irradiation. It is, therefore, unclear how countermeasures to accidental exposure to high dose whole body irradiation in humans or bone marrow transplantation following radiation-induced bone marrow ablation in animals influence bone metabolism.

The goals of the present studies were to evaluate the early effects of acute whole body γ-irradiation on bone metabolism in a mouse model and determine whether the anticipated detrimental effects of a challenging high-dose irradiation are attenuated by prior exposure to a relatively low dose of priming radiation. In addition, we investigated the efficacy of bone marrow transplantation in reversing the long-duration skeletal effects of high-dose whole body γ-irradiation.

2. Materials and Methods

Male and female C57BL/6 (B6) mice were used in the irradiation experiments (see Experiment 1-4 below) and female C57BL/6-Tg(CAG-EGFP)1Osb/J mice with constitutive expression of green fluorescent protein (GFP) were used in the cell tracking experiment (see Experiment 5 below). Mice were purchased from Jackson Laboratory (Bar Harbor, Maine). The mice were housed individually in a temperature (21-23°C) and light (12 hr light dark cycle) controlled room. Food and water were provided *ad libitum* to all animals. The mice were maintained in accordance with the NIH Guide for the Care and the Use of Laboratory Animals and the Institutional Animal Care and Use Committee at the Johnson Space Center (Experiments 1-3) and Oregon State University (Experiments 4-5) approved the experimental protocols.

2.1 Experimental Design

Experiments were performed to assess the efficacy of radioprotection on bone and to evaluate the effects of bone marrow transplantation in mitigating whole body γ-radiation-induced adverse skeletal effects. In the radioadaptive study, 0.5 milligray (mGy) of radiation was used as a priming dose, followed by 6 Gy as the challenging dose, whereas 9 Gy was used in the bone marrow transplantation study. If untreated, approximately 50% of the mice would be expected to die within 30 days following whole body γ-irradiation with a dose of 6 Gy [18]. A dose of 9 Gy without treatment would be expected to result in 100% mortality [19].

2.1.1 Efficacy of Radioprotection on Bone

Experiment 1 was performed to characterize the effects of whole body γ-irradiation (using a ^{137}Cs source located at NASA Johnson Space Center, Houston, Texas) on bone architecture and cellular indices of bone formation and resorption. Two-month-old male B6 mice were divided into 4 groups (n=6/group): 1) untreated control, 2) irradiated with a priming dose of 0.5 mGy, 3) irradiated with a challenging dose of 6 Gy, or 4) irradiated with 0.5 mGy followed 24 hours later by irradiation with 6 Gy. The mice were sacrificed 14 days following the last irradiation. For tissue collection, animals were anesthetized with 2-3% isofluorane delivered in oxygen and death was induced by decapitation with a guillotine. Tibiae and 5^{th} lumbar vertebrae were removed and stored in 70% ethanol for micro-computed tomography (CT) and/or bone histomorphometric analysis.

Experiments 2 and 3 were conducted to further characterize the cellular mechanisms responsible for whole body γ-radiation-induced changes in bone architecture. The treatment groups were the same as in Experiment 1, but mice were sacrificed 1 day (Experiment 2; n=6/group) or 3 days (Experiment 3; n=3/group) following irradiation. Tissues were collected as in Experiment 1.

2.1.2 Efficacy of Bone Marrow Transplantation on Bone

Experiment 4 was performed to assess the efficacy of bone marrow transplantation following lethal (9 Gy) whole body γ-irradiation on bone mass and turnover. Two-month-old female B6 mice were randomized by weight into 3 groups: baseline control (n= 9), untreated (n=7) and irradiated bone marrow recipients + donor bone marrow (B6→B6) (n=7). For bone marrow transplantation, bone marrow cells were isolated from femurs and tibias of donor mice by flushing the bones with phosphate buffered saline using a sterile 3ml syringe fitted with a 24G needle. Bone marrow cells were made into single cell suspensions by repeated pipetting. To facilitate accurate cell count of nucleated cells, red blood cells in the bone marrow were selectively removed by incubating with red blood cell lysis buffer (150 mM NH4Cl, 1 mM KHCO3, 0.1 mM EDTA, pH 7.2) per standard immunology procedure which have been shown to be compatible with bone marrow transplantation. After lysing of red blood cells, bone marrow cells were resuspended to 5×10^7 cells/ml in PBS for bone marrow transplantation.

Transplant recipients were lethally irradiated at 9 Gy using a ^{60}Co irradiator source (Radiation Center, Oregon State University) and reconstituted with 1×10^7 donor bone marrow cells by injection (200 µl) in the tail vein. Baseline control mice were labeled with the fluorochrome calcein (15 mg/kg) 4 and 1 days prior to sacrifice at 8 weeks of age. The remaining mice were maintained for 9 weeks following bone marrow engraftment, labeled with calcein (15 mg/kg) 4 and 1 days prior to sacrifice, and sacrificed at 17 weeks of age. Additionally (Experiment 5), a group of B6 mice (n=4) was engrafted with bone marrow from GFP mice to track cell repopulation in different tissues. Bone marrow transplantation results in a chimera with donor-derived and recipient cells. The use of GFP bone marrow serves as an important internal control to definitely define and quantitate donor-derived cells versus recipient cells. For tissue collection, mice were anesthetized with 2-3% isofluorane delivered in oxygen and death was induced by cardiac excision. Uteri were removed and weighed. Right femora and lumbar vertebrae were removed and stored in 70% ethanol for CT and/or histomorphometric analysis. Spleens and left femora were immediately processed for cell measurements.

2.2 Micro-computed tomography

µCT was used for nondestructive 3-dimensional evaluation of bone volume and architecture. Long bones (tibia for Experiment 1 and femur for Experiment 4) and lumbar vertebrae (Experiments 1 and 4) were scanned using a Scanco CT40 scanner (Scanco Medical AG, Basserdorf, Switzerland) at a voxel size of 12 m × 12 m × 12 m. The threshold value for evaluation was determined empirically and set at 245 (gray scale, 0-1000). Entire tibia (cancellous + cortical bone) was evaluated followed by evaluation of cortical bone at the midshaft and cancellous bone in the proximal metaphysis. For the tibial midshaft, 20 slices (240 m in length) of bone were evaluated and total cross-sectional volume (cortical and marrow volume, mm^3), cortical volume (mm^3), marrow volume (mm^3), and cortical thickness (m) were measured. Maximum (I_{max}), minimum (I_{min}), and polar (I_{polar}) moment of inertias were calculated as surrogate measures of bone strength in bending (I_{max} and I_{min}) and torsion (I_{polar}). For the tibial metaphysis, 40 slices (480 µm in length) of cancellous bone were evaluated. Similar measurements were performed for the femur, with the exception that the distal femoral metaphysis (40 slices) and epiphysis (entire region of secondary spongiosa) were evaluated.

Analysis of the lumbar vertebra included the entire region of secondary spongiosa between the cranial and caudal growth plates. Direct cancellous bone measurements in the proximal tibia metaphysis/distal femur metaphysis/distal femur epiphysis and lumbar vertebra included cancellous bone volume fraction (bone volume/tissue volume, volume of total tissue occupied by cancellous bone, %), connectivity density (number of redundant connections per unit volume, mm^{-3}; this index detects defects in cancellous architecture), trabecular thickness (mean thickness of individual trabeculae, m), trabecular number (number of trabecular intersects per distance, mm^{-1}), and trabecular separation (the distance between trabeculae, m).

2.3 Histomorphometry

Lumbar vertebrae were prepared for histomorphometric evaluation as described [20]. Sections were stained according to the Von Kossa method with a tetrachrome counter stain (Polysciences, Warrington, PA) for assessment of bone area and cell-based measurements. Unstained sections were used for assessment of dynamic histomorphometry. Histomorphometric data were collected using the OsteoMeasure System (OsteoMetrics, Inc., Atlanta, GA). Static cancellous bone endpoints (Experiments 1-4) included bone area fraction (bone area/tissue area, %) and the derived architectural indices of trabecular number (mm^{-1}), trabecular thickness (μm), and trabecular separation (μm). Osteoblast and osteoclast perimeters were measured and expressed as % of total bone perimeter and nucleated cells were measured and expressed as marrow cell density. Fluorochrome-based indices of bone formation (Experiment 4) included mineralizing perimeter (percentage of bone with double label + ½ single label) and mineral apposition rate (mean distance between two fluorochrome markers that comprise a double label divided by interlabel time, μm/d). Bone formation rate was calculated using a bone perimeter referent ($\mu m^2/\mu m/y$). Additional cell measurements (Experiment 4) were performed in toluidine blue-stained sections and included megakaryocyte and adipocyte density. Megakaryocytes were measured because radiation-induced thrombocytopenia plays a role in radiation mortality [21]. Bone marrow adipocytes were measured because radiation is associated with increased deposition of fat into bone marrow [22]. Morphologically, megakaryocytes were identified as large cells with a multilobed nucleus. Adipocytes were identified as large circular or oval shaped cells, bordered by a prominent cell membrane and deficient in cytoplasmic staining due to alcohol extraction of intracellular lipids during processing. All data are reported using standard nomenclature.

2.4 Fluorescence Activated Cell Sorting Analysis

Spleens and bone marrow flushed from the femurs of individual mice were made into single cell suspensions. Red blood cells were removed by incubating with red blood cell lysis buffer per standard immunology protocol for the preparation of cells for flow cytometry. Cells were resuspended in flow cytometry buffer (PBS, 2% FBS, 1mM EDTA), and incubated for 30 mins on ice in the dark with antibodies specific against CD4, CD8, CD11b, CD19, CD117 (c-Kit) (eBiosciences, San Diego, CA), CD115 (MCSF receptor) (Serotec, Raleigh, NC), and a lineage cell (lin) detection cocktail (Miltenyi Biotech, Auburn, CA). The cocktail is comprised of a panel of monoclonal antibodies that detect lineage-committed immune cell populations including T cells, B cells, monocytes/macrophages, granulocytes, and erythrocytes, and distinguish these from the lineage-negative stem cell and progenitor cell compartments. After extensive washing, cells were resuspended in buffer for flow cytometry analysis. Data were acquired using FACSCalibur (BD Biosciences, San Jose, CA). Data analyses were performed using Summit software (DakoCytomation, Fort Collins, CO). GFP donor-derived immune cells were identified based on the expression of GFP in combination with the following cell surface markers: T cells ($CD4^+$ or $CD8^+$), B cells ($CD19^+$), osteoclast precursors ($CD11b^+$ MCSF $receptor^+$), hematopoietic stem cells ($lin^-cKit^+Sca1^+$) and mesenchymal stem cells ($lin^-cKit^-Sca1^+$).

2.5 Statistical Analysis

Multivariate analysis of variance (MANOVA) was used to test for equal means across radiation dose for the collection

of variables within the response categories of total tibia, midshaft tibia, proximal tibia metaphysis, and lumbar vertebra. For each of the four MANOVA tests, the null hypothesis of equal mean vectors across the control, 0.5 mGy, 6 Gy, and sequential 0.5 mGy + 6Gy dose levels was tested using Wilks' lambda statistic. When significant differences were found between mean vectors, follow-up statistical tests were performed using one-way analysis of variance (ANOVA) to compare the dose groups for individual variables, and t-tests were used for two-group comparisons. Linear contrasts that define interactions and two-group comparisons were tested using MANOVA with Wilks' lambda or F-tests in ANOVA.

Separate two-factor ANOVA models were fit to the endpoints osteoclast-lined bone perimeter, osteoblast-lined bone perimeter, and marrow cell density. The factor variables in each model were treatment group (control, 0.5 mGy, 6 Gy, and sequential 0.5 mGy + 6 Gy) and day (day 1, day 3, and day 14). Results were stratified by day if a treatment by day interaction effect was statistically significant according to a F test. Otherwise, a model with main effects was reported. Adjusting for day, F tests of linear contrasts were performed to compare the 0.5 mGy and 6 Gy dose groups to the control group, and to investigate for an interaction effect of the sequential dosage.

The individual variables in the endpoint groups of total femur, midshaft femur, distal femur metaphysis, distal femur epiphysis, and lumbar vertebra, as well as bone and hematopoietic lineage cells, and dynamic indices of bone formation were analyzed using separate MANOVA models. For each endpoint group, the null hypothesis of equal means across the baseline, control, and 9 Gy irradiation + bone marrow transplantation categories was tested using Wilks' Lambda statistic. When significant differences were found using MANOVA, follow-up ANOVA F-tests were performed on individual variables, and linear contrasts were tested to determine differences among categories. Conditions for use of ANOVA models were assessed by Bartlett's test for homogeneity of variance and normal quantile plots. The modified F* test [23] was used when the assumption of equal variance was violated, with Welch's two-sample t-test used for pairwise comparisons. Adjustment for multiple comparisons was made by constraining the false discovery rate to be at most 5%. Differences were considered significant at adjusted $p < 0.05$. Data are expressed as mean ± SE. Statistical analysis was performed using Stata version 10 (StataCorp LP, College Station, Texas).

3. Results

3.1 Efficacy of Radioprotection on Bone

The efficacy of a radioconditioning priming dose of 0.5 mGy in preventing detrimental changes in bone mass and architecture in tibia and lumbar vertebra 14 days following exposure to a challenging dose of 6 Gy was evaluated by μCT, and results are presented in Table 1. Tibial length, total tibial bone volume, and cortical bone parameters (cross-sectional volume, cortical volume, marrow volume, cortical thickness, I_{Max}, I_{Min}, and I_{Polar}) did not differ, on average, with treatment. In contrast, proximal tibial metaphysis cancellous bone volume fraction (bone volume/tissue volume), connectivity density and trabecular number were lower while trabecular thickness and separation were higher in mice

subjected to the 6 Gy challenging dose. The 0.5 mGy priming dose used for radioconditioning had no significant effect on tibial cortical or cancellous bone mass or architecture ($p = 0.83$) nor did the 0.5 mGy priming dose affect tibial bone response to the challenging dose of 6 Gy ($p = 0.80$).

Table 1.

Effects of a radioconditioning priming dose of 0.5 mGy in preventing detrimental changes in bone mass and architecture in tibia and lumbar vertebra following exposure to a challenging radiation dose of 6 Gy. Seven-week-old mice were treated with either a priming dose of radiation (0.55 mGy), a challenging dose radiation (6 Gy), or a priming dose of radiation to induce radioconditioning followed 1 day later by a challenging dose of radiation (0.5 mGy + 6 Gy, combination) and sacrificed 14 days later.

	Radiation Dose				
Endpoint	**Control**	**0.5 mGy (priming Dose)**	**6 Gy (Challenging Dose)**	**0.5 mGy, 6 Gy**	**FDR-Adjusted P-value***
Total Tibia					
Length (mm)	18.0 ± 0.1	18.0 ± 0.1	17.7 ± 0.1	17.8 ± 0.1	NS
Bone volume (mm^3)	16.7 ± 0.7	16.5 ± 0.4	16.5 ± 0.6	16.4 ± 0.5	NS
Midshaft Tibia (cortical bone)					
Cross-sectional volume (mm^3)	0.23 ± 0.02	0.22 ± 0.01	0.22 ± 0.01	0.22 ± 0.02	NS
Cortical volume (mm^3)	0.16 ± 0.01	0.15 ± 0.00	0.15 ± 0.01	0.15 ± 0.01	NS
Marrow volume (mm^3)	0.07 ± 0.00	0.06 ± 0.00	0.07 ± 0.00	0.07 ± 0.00	NS
Cortical thickness (μm)	242 ± 13	242 ± 6	234 ± 7	233 ± 10	NS
I_{Max} (mm^4)	0.09 ± 0.02	0.08 ± 0.00	0.08 ± 0.01	0.08 ± 0.01	NS
I_{Min} (mm^4)	0.06 ± 0.01	0.05 ± 0.00	0.05 ± 0.01	0.06 ± 0.01	NS
I_{polar} (mm^4)	0.15 ± 0.03	0.13 ± 0.01	0.14 ± 0.02	0.14 ± 0.02	NS
Proximal Tibia Metaphysis (cancellous bone)					
Bone volume/Tissue volume (%)	13.9 ± 0.5	11.7 ± 0.7	8.2 ± 0.7[a]	9.1 ± 0.9	<0.0014 <0.001

Endpoint	Radiation Dose				FDR-Adjusted P-value*
	Control	0.5 mGy (priming Dose)	6 Gy (Challenging Dose)	0.5 mGy, 6 Gy	
Connectivity density (mm^{-3})	172 ± 12	138 ± 18	43 ± 6[a]	56 ± 15	4
					<0.001
Trabecular number (mm^{-1})	6.3 ± 0.1	6.1 ± 0.2	4.6 ± 0.2[a]	4.6 ± 0.2	4
					<0.001
Trabecular thickness (mm)	41 ± 1	39 ± 0	45 ± 1[a]	46 ± 1	4
					<0.001
Trabecular separation (mm)	156 ± 3	161 ± 5	216 ± 8[a]	214 ± 9	4
Lumbar Vertebra (cancellous bone)					
Bone volume/Tissue volume (%)	17.2 ± 0.5	15.7 ± 0.6	14.2 ± 0.6	15.1 ± 1.2	0.093
					<0.001
Connectivity density (mm^{-3})	254 ± 10	258 ± 7	132 ± 9[a]	144 ± 12	4
Trabecular number (mm^{-1})	5.4 ± 0.1	5.5 ± 0.1	4.9 ± 0.1[a]	4.9 ± 0.1	<0.001
					4
					<0.001
Trabecular thickness (mm)	38 ± 1	37 ± 1	43 ± 1[a]	44 ± 2	4
					<0.001
Trabecular separation (mm)	180 ± 3	179 ± 4	203 ± 5[a]	202 ± 6	4

Open in a new tab

Data are mean ± SE

*P values were adjusted upward using the false discovery rate (FDR) method to account for multiple comparisons

[a]Significantly different from Control

Connectivity density and trabecular number were also lower, while trabecular thickness and separation were higher in lumbar vertebra of mice subjected to the 6 Gy challenging dose. Also, as in the proximal tibial metaphysis, the priming dose of radiation used to induce radioconditioning had no significant effect on vertebral cancellous bone mass or architecture ($p = 0.57$) and there was no interaction between the priming dose and challenging dose for any of the vertebral cancellous endpoints evaluated ($p = 0.59$).

The effects of radiation on osteoblast-lined and osteoclast-lined bone perimeter and on bone marrow cell density in lumbar vertebra are shown in Figures 1 and 2. A statistically significant interaction ($p = 0.002$) was identified between treatment and time for osteoblast-lined bone perimeter. Compared to time-matched controls, osteoblast-lined bone perimeter was 290% higher at 1 day ($p = 0.04$), 1230% higher at 3 days ($p < 0.0001$), and 530% higher at 14 days ($p = 0.003$) following irradiation at 6 Gy (Figure 1 A-C). Significant differences in osteoblast-lined bone perimeter due to priming dose were not detected at any time point. Osteoblast-lined bone perimeter was higher on day 14 post-irradiation in mice receiving the 0.5 mGy priming dose followed by the 6 Gy challenging dose compared to mice receiving the 6 Gy dose alone. Osteoclast-lined bone perimeter was higher in mice receiving the 6 Gy challenging dose than in control mice, irrespective of time (Figure 1 D-F). A statistically significant effect on osteoclast-lined bone perimeter of the 0.5 mGy priming dose was not detected nor was there a difference in response to 6 Gy *versus* 0.5 mGy followed by 6 Gy irradiation. A significant interaction ($p = 0.017$) was identified between treatment and time for bone marrow cell density. Compared to time-matched controls, bone marrow cell density was 77% lower at 1 day ($p < 0.0001$), 86% lower at 3 days ($p < 0.0001$), and 30% lower at 14 days ($p = 0.0025$) following the 6 Gy challenging dose (Figure 1 G-I). There was a strong association between radiation-induced marrow cell death and activation of bone lining cells to express the osteoblast phenotype (Pearson correlation −0.85, $p<0.0001$). Significant differences in marrow cell density due to priming dose were not detected at any time point. Marrow cell density was lower on day 14 post-irradiation in mice receiving a 0.5 mGy priming dose followed by the 6 Gy challenging dose compared to mice receiving the 6 Gy dose alone. Representative micrographs illustrating the dramatic effects of the challenging radiation dose of 6 Gy on osteoblast-lined bone perimeter and marrow cellularity are shown in Figure 2.

Figure 1.

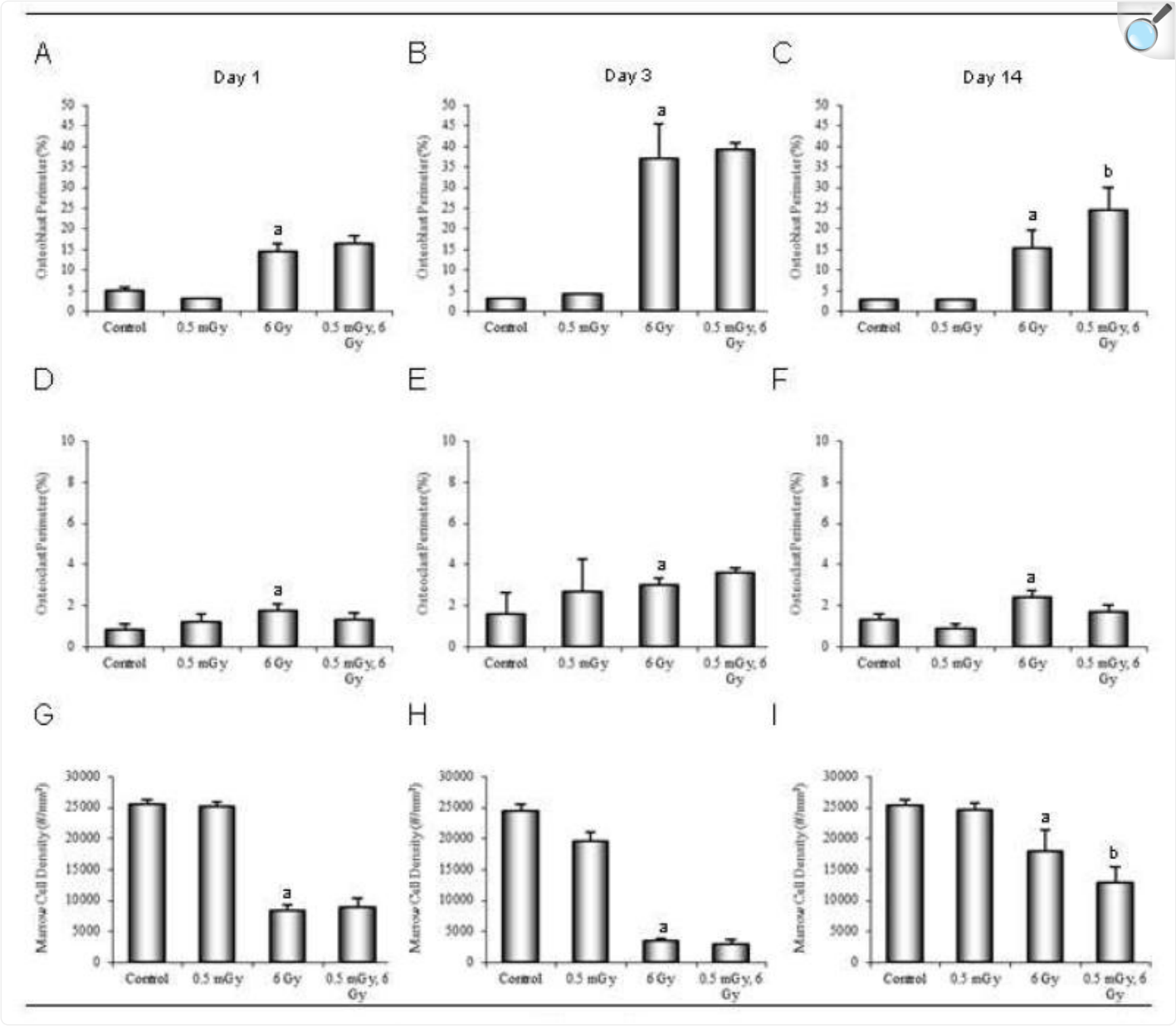

Open in a new tab

Efficacy of a priming dose (0.5 mGy) of radiation in ameliorating the detrimental effects of a challenging dose (6 Gy) of radiation in lumbar vertebrae. High dose radiation results in rapid increase in osteoblast (A-C) and osteoclast-lined bone perimeter (D-F) in spite of reduction in marrow cell density (G-I). Data are mean ± SE (n = 6/group for day 1, 3/group for day 3, and 6/group for day 14). [a]Significantly different from Control; [b]Significantly different from 6 Gy.

Figure 2.

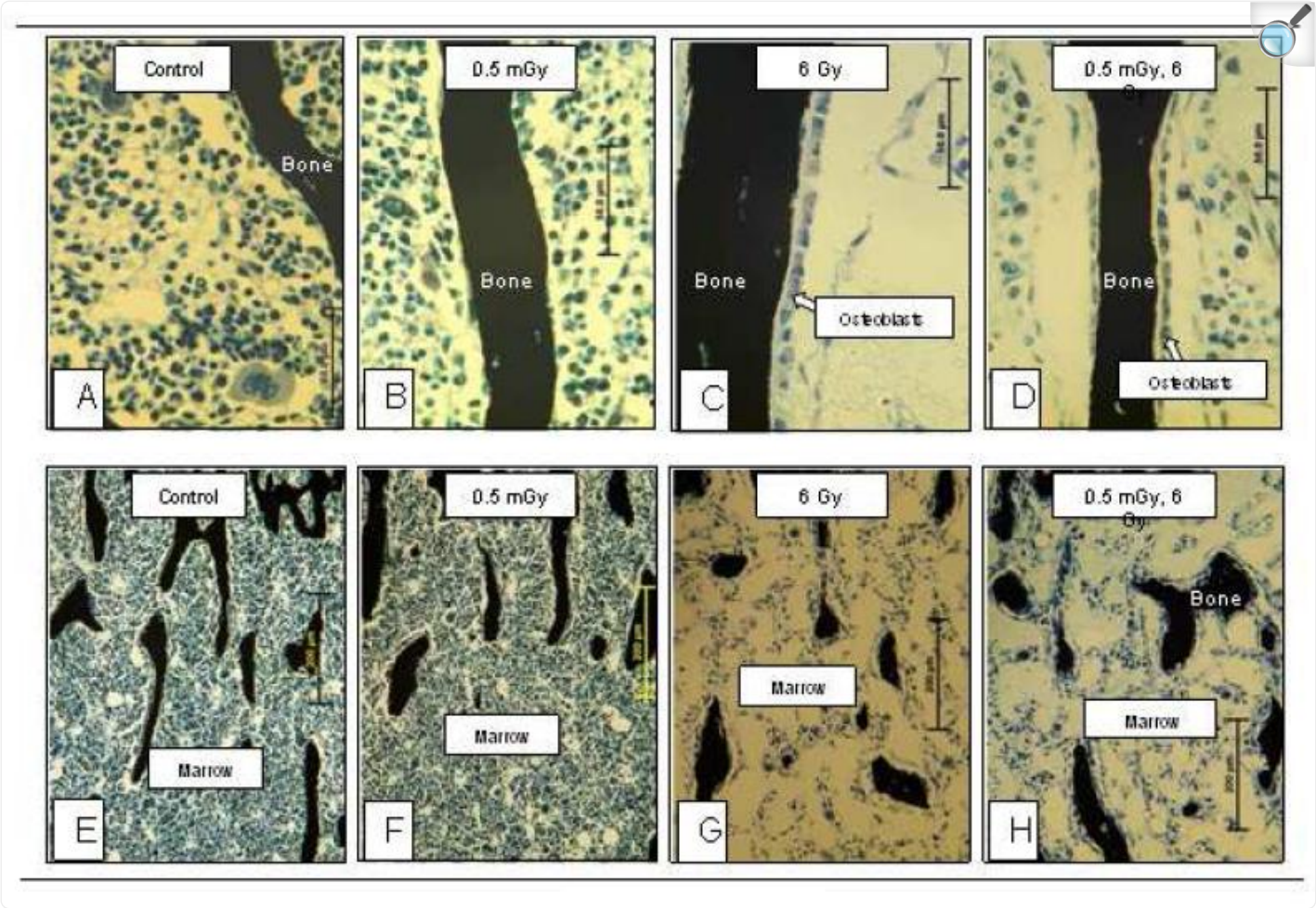

Open in a new tab

Representative photomicrographs of osteoblasts (A-D) and marrow cells (E-H) in mice irradiated with a priming dose (0.5 mGy) 24 hrs prior to a challenging dose (6 Gy) of radiation. Please note the dramatic increase in osteoblast-lined bone perimeter and drastic reduction in marrow cell density with challenging dose (6 Gy) irradiation.

3.2 Efficacy of Marrow Transplantation Following Irradiation on Bone

The effects of age and lethal whole-body γ-irradiation (9 Gy) followed by bone marrow transplantation on bone mass and architecture in the femur and lumbar vertebra, as determined by μCT, are shown in Table 2. Femoral length, total femoral bone volume, cortical volume and cortical thickness increased while marrow volume decreased with age (8-

week-old baseline mice *versus* 17-week-old control mice). Significant differences in cross-sectional volume and moments of inertia were not detected with age. In addition, significant differences between control and bone marrow-transplanted mice (transplanted at 8 weeks of age and sacrificed 9 weeks later) were not detected for total femoral bone volume or any of the cortical endpoints evaluated. In contrast, femoral length was lower in the bone marrow-transplanted mice compared to control mice.

Table 2.

Effects of bone marrow cell transplantation (BMT) on bone mass and architecture in femur and lumbar vertebra. Eight-week-old mice were lethally irradiated (9 Gy), transplanted with donor bone marrow cells, and sacrificed 9 weeks later at 17 weeks of age.

	8-week-old	17-week-old		FDR-Adjusted P-value*
Endpoint	**Baseline**	**Control**	**9 Gy + BMT**	
Total Femur				
Length (mm)	14.5 ± 0.1	15.5 ± 0.1[a]	15.1 ± 0.1[a,b]	0.0007
Bone volume (mm^3)	15.7 ± 0.3	18.1 ± 0.5[a]	17.2 ± 0.3[a]	<0.0003
Midshaft Femur (cortical bone)				
Cross-sectional volume (mm^3)	0.37 ± 0.00	0.35 ± 0.01	0.34 ± 0.01[a]	0.0497
Cortical volume (mm^3)	0.15 ± 0.00	0.17 ± 0.00[a]	0.17 ± 0.00[a]	0.0003
Marrow volume (mm^3)	0.22 ± 0.00	0.18 ± 0.01[a]	0.17 ± 0.01[a]	<0.0003
Cortical thickness (μm)	167 ± 2	201 ± 4[a]	204 ± 2[a]	<0.0003
I_{Max} (mm^4)	0.21 ± 0.00	0.22 ± 0.01	0.21 ± 0.01	NS
I_{Min} (mm^4)	0.10 ± 0.00	0.10 ± 0.00	0.10 ± 0.00	NS
I_{polar} (mm^4)	0.31 ± 0.00	0.32 ± 0.01	0.31 ± 0.02	NS
Distal Femur Metaphysis (cancellous bone)				
Bone volume/Tissue volume (%)	9.8 ± 0.6	3.8 ± 0.9[a]	2.7 ± 0.4[a]	<0.0003
Connectivity density (mm^{-3})	100 ± 9	17 ± 7[a]	10 ± 4[a]	<0.0003
Trabecular number (mm^{-1})	5.4 ± 0.1	3.8 ± 0.1[a]	3.4 ± 0.1[a,b]	<0.0003
Trabecular thickness (μm)	38 ± 1	41 ± 2	44 ± 1[a]	0.0588
Trabecular separation (μm)	186 ± 3	273 ± 7[a]	309 ± 6[a,b]	<0.0003

Endpoint	8-week-old	17-week-old		FDR-Adjusted P-value*
	Baseline	Control	9 Gy + BMT	
Distal Femur Epiphysis (cancellous bone)				
Bone volume/Tissue volume (%)	27.1 ± 0.7	25.4 ± 1.2	23.8 ± 0.5[a]	0.0497
Connectivity density (mm^{-3})	207 ± 8	104 ± 9[a]	78 ± 3[a,b]	<0.0003
Trabecular number (mm^{-1})	6.6 ± 0.2	5.4 ± 0.1[a]	5.2 ± 0.2[a]	0.0003
Trabecular thickness (μm)	55 ± 1	64 ± 2[a]	66 ± 1[a]	<0.0003
Trabecular separation (μm)	161 ± 4	202 ± 6[a]	199 ± 7[a]	<0.0003
Lumbar Vertebra (cancellous bone)				
Bone volume/Tissue volume (%)	15.7 ± 0.7	15.2 ± 1.1	10.8 ± 0.4[a,b]	0.0003
Connectivity density (mm^{-3})	203 ± 9	160 ± 29	71 ± 4.8[a,b]	0.0028
Trabecular number (mm^{-1})	4.7 ± 0.1	3.9 ± 0.2[a]	3.4 ± 0.0[a]	0.0003
Trabecular thickness (μm)	41 ± 1	45 ± 1[a]	45 ± 1[a]	0.016
Trabecular separation (μm)	214 ± 5	265 ± 14[a]	294 ± 3[a]	0.0007

Data are mean ± SE

*P values were adjusted upward using the false discovery rate (FDR) method to account for multiple comparisons

[a]Significantly different from Baseline

[b]Significantly different from Control

Distal femur metaphysis cancellous bone volume fraction, connectivity density and trabecular number decreased, trabecular separation increased, while differences in trabecular thickness were not detected between 8-week-old baseline mice and 17-week-old control mice. Significant differences between control mice and bone marrow-transplanted mice were not detected for cancellous bone volume fraction, connectivity density, or trabecular thickness. However, trabecular number was lower and trabecular separation was higher in bone marrow-transplanted compared to control mice.

Distal femur epiphysis connectivity density and trabecular number decreased with age, trabecular thickness and separation increased with age, while differences in cancellous bone volume fraction were not detected with age between the 8-week-old baseline and 17-week-old control mice. With the exception of connectivity density, which was lower in bone marrow-transplanted compared to control mice, significant differences between the two groups were not detected for any cancellous endpoint evaluated in the distal femur epiphysis.

Vertebral trabecular number decreased, trabecular thickness and separation increased, while differences in cancellous bone volume fraction and connectivity density were not detected with age between the 8-week-old baseline and 17-week-old control mice. Cancellous bone volume fraction and connectivity density were lower in bone marrow-transplanted mice compared to control mice. Significant differences between control mice and bone marrow-transplanted mice were not detected for any other endpoints evaluated.

Osteoblast-lined bone perimeter, osteoclast-lined bone perimeter, mineralizing perimeter, mineral apposition rate, bone formation rate, marrow cell density, and megakaryocyte density in lumbar vertebra, and cell tracking at 9 weeks following exposure to a lethal (9 Gy) dose of radiation and subsequent bone marrow transplantation are shown in Figures 3 and 4, respectively. Significant differences in osteoblast and osteoclast-lined bone perimeter, dynamic indices of bone formation, marrow cell density, or megakaryocyte density were not detected with age or between control mice and irradiated mice transplanted with bone marrow cells (Figure 3). Adipocytes were rarely observed in lumbar vertebrae of either control or irradiated mice.

Figure 3.

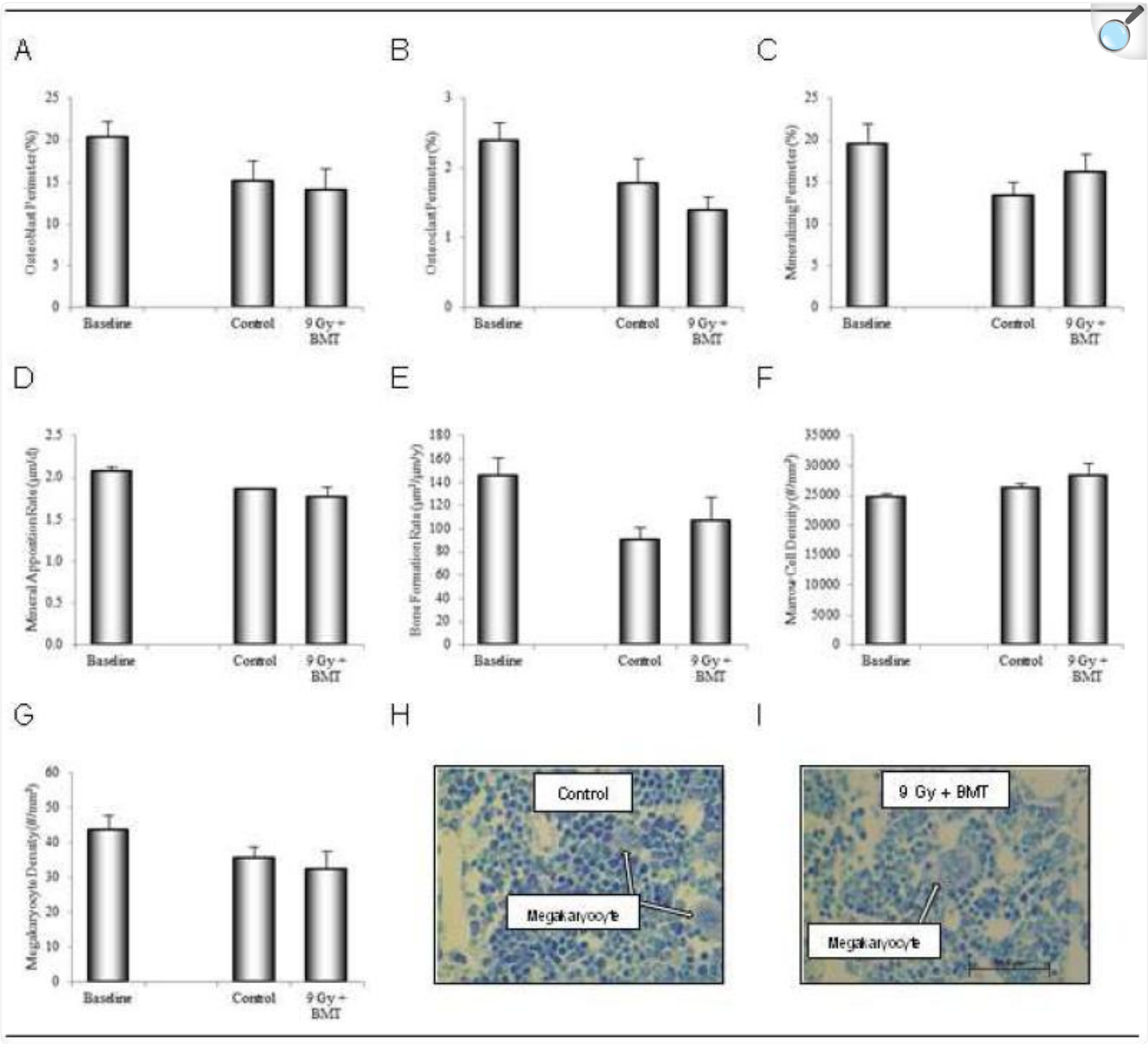

Open in a new tab

Bone marrow transplantation (BMT) normalizes indices of bone turnover in lumbar vertebrae in lethally irradiated (9 Gy) mice. Please note the lack of differences between control and BMT mice for osteoblast-lined bone perimeter (A), osteoclast-lined bone perimeter (B), mineralizing bone perimeter (C), mineral apposition rate (D), bone formation rate (E), marrow cell density (F) and megakaryocyte density (G) 9 weeks following lethal irradiation and BMT. Representative photomicrographs of marrow from a control and irradiated bone marrow-transplanted mouse 9 weeks following transplantation is shown in H and I, respectively. Data are

mean ± SE (n = 5/group).

Figure 4.

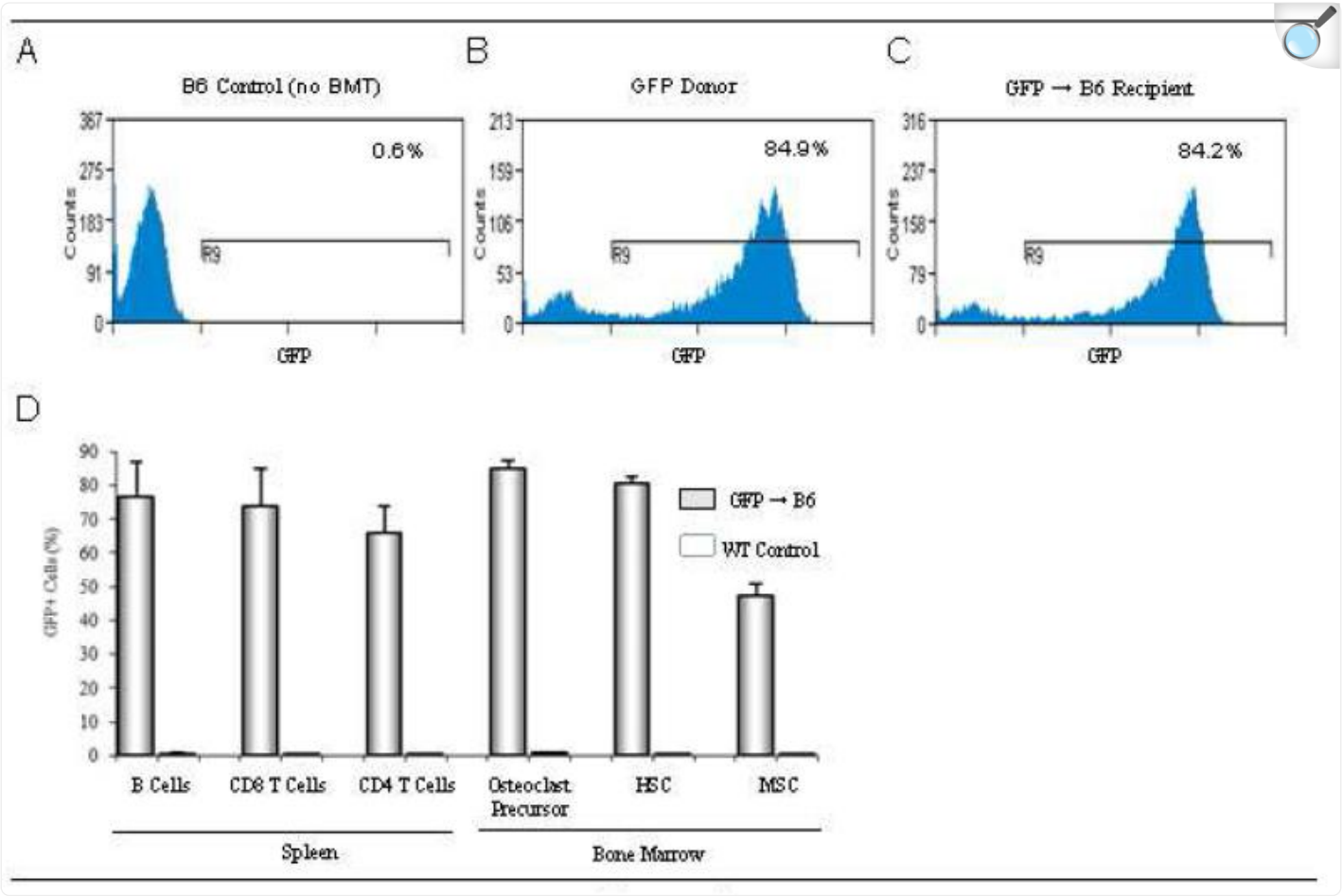

Open in a new tab

Reconstitution of donor-derived GFP$^+$ cells in bone marrow transplantation (BMT) recipients. Representative flow cytometry plots showing the percentages of GFP$^+$ B cells in the spleens of B6 control mouse (A), GFP donor mouse (B), and GFP → B6 recipient (C) 9 weeks following lethal irradiation and BMT. Frequencies of various donor-derived GFP$^+$ cells in the spleens and bone marrow of GFP → B6 recipients (D). HSC = hematopoietic stem cells, MSC = mesenchymal stem cells. Data are mean ± SE (n = 3/group).

As expected, GFP expression was not detected in hematopoietic or mesenchymal lineage cells obtained from B6 control mice (Figure 4). The great majority of immune cells in spleen (B cells, CD8 T cells, and CD4 T cells) and early

osteoclast precursors in bone marrow ($MCFR^+$ $CD11b^+$) of irradiated animals transplanted with bone marrow from GFP expressing mice expressed GFP (Figure 4). Approximately 50% of the mesenchymal lineage cells obtained from bone marrow of whole body γ-irradiated animals transplanted with bone marrow from GFP expressing mice expressed GFP (Figure 4).

4. Discussion

A 6 Gy whole-body dose of γ-radiation resulted in a rapid decline in bone marrow cell density. Despite the overall dramatic reduction in marrow cellularity, cellular indices of bone formation and resorption were increased. The increase in osteoblast-lined bone perimeter was particularly notable and was well established within 1 day of irradiation. The increase in bone turnover resulted in decreased cancellous bone volume fraction, manifested as a decrease in trabecular number that was partially offset by a simultaneous increase in trabecular thickness. As a consequence, important indices of bone quality (e.g., connectivity density) were more negatively impacted by radiation than would have been anticipated solely by the reduction in cancellous bone volume fraction. A radioconditioning priming dose (0.5 mGy) administered 24 hrs prior to administration of a challenging dose (6 Gy) was overall ineffective in moderating the effects of challenging irradiation on bone cell populations or bone architecture. Bone marrow transplantation following lethal (9 Gy) irradiation resulted in quantitative replacement of host bone marrow hematopoietic cells with donor cells, normalized bone marrow cell density, normalized indices of bone turnover, preserved normal cortical bone architecture and limited radiation-induced deterioration of cancellous bone architecture.

Radiation-induced cancellous osteopenia was associated with a dramatic increase in osteoblast-lined bone perimeter. This increase was observed within 1 day of exposure to challenging dose irradiation. This rapid response contrasts with the much longer duration required for osteoblasts to differentiate from their mesenchymal stromal cell progenitors residing within bone marrow [24]. The timing of the increase in osteoblast-lined bone perimeter following challenging dose irradiation is consistent with activation of bone lining cells. Also consistent with activation of bone lining cells is the increase in trabecular thickness noted 14 days following irradiation. Bone lining cells are post-mitotic osteoblast lineage cells that line inactive bone surfaces and as such are typically much more numerous than osteoblasts. Bone lining cells can be quickly activated by hormones and growth factors such as parathyroid hormone, growth hormone and basic fibroblast growth factor to express the osteoblast phenotype [25, 26]. The studies reported here indicate that lining cells are also activated by 6 Gy of whole-body γ-radiation.

The short-term effects of high-dose whole-body γ-radiation on bone metabolism have received little attention. However, similar to our findings, Dominici et al. [27] reported a rapid increase in osteoblasts following lethal (11 Gy) whole body irradiation. In contrast, a recent study reported a low level of bone formation following irradiation with a sublethal 5 Gy dose [10]. As in our study, sublethal irradiation resulted in decreased trabecular number but increased trabecular thickness, suggesting that a prior undetected increase in bone formation had indeed occurred. Osteoblast-lined bone perimeter was not reported in the Green and colleagues study [10] and the fluorochrome labeling protocol used to

calculate bone formation at later time points may have resulted in excessive label escape error, potentially compromising interpretation of dynamic bone measurements [28].

The lower cancellous bone volume observed 14 days following irradiation in our study and a similar decrease reported by Green et al. [10] suggest that increased bone resorption ultimately predominates over the simultaneous increase in bone formation. Osteoclasts are derived from hematopoietic stem cells residing within bone marrow [29, 30]. Osteoclast precursors have a long lifespan in circulation [31]. As a consequence, proliferation would not be required for the increase in osteoclast perimeter following irradiation observed in this and earlier studies [32]. In adults, bone formation during bone remodeling is coupled spatially and temporally, but not necessarily in magnitude, to prevailing levels of bone resorption. An increase in bone resorption such as that occurring following menopause in women or ovariectomy in skeletally mature rats results in a coupled, although lesser, increase in bone formation [33]. However, the rapid radiation-induced increase in osteoblasts in lumbar vertebra supports another mechanism, namely activation of bone lining cells. Whereas coupled bone remodeling would tend to preserve bone architecture, the absence of coupling between bone resorption and bone formation observed in this study acts to accentuate changes in bone architecture (increased trabecular thickness and reduced trabecular number) in irradiated mice because the increases in bone formation and resorption are occurring at discrete sites.

The negative impact of high dose radiation on bone marrow became recognized when several of the most prominent early workers in the field of radiochemical research died of radiation-induced hematological diseases, including aplastic anemia and leukemia [34]. Whereas proliferating cells are highly sensitive to radiation, post-mitotic bone cells are resistant to radiation-induced cell death. Activation of bone lining cells and osteoclast formation from circulating osteoclast precursors represent post-mitotic cell differentiation. The mechanism for the increased bone turnover following irradiation is likely directly related to bone marrow failure. Plausible, non-mutually exclusive mechanisms include: 1) activation of osteoblasts and recruitment of osteoclast precursors from blood by factors released from bone marrow cells in response to radiation and/or 2) failure of dying marrow cells to produce factors that inhibit bone turnover.

Bone lining cell activation is reversible. Rapid reversal of osteoblasts to bone lining cells occurs once stimulatory factors are withdrawn [35]. In the present study, marrow cell depletion occurred within 1 day following irradiation and partially rebounded by 14 days. High dose irradiation results in a rapid increase in gene expression for platelet derived growth factor-β and basic fibroblast growth factor [27], providing a potential mechanism for the radiation-induced increase in osteoblasts because these growth factors have been implicated in the bone lining cell to osteoblast transition [26, 36]. However, bone marrow ablation, a method that removes bone marrow cells, also induces a dramatic bone turnover response [37, 38]. Bone turnover is regulated by hematopoietic cells [39, 40] and hematological disorders such as anemia result in skeletal disorders [41, 42]. Thus, hematopoietic cells may inhibit transition of lining cells to osteoblasts. As such, loss of this negative regulation by hematopoietic lineage cells is a plausible alternative mechanism for increased bone turnover following irradiation. An important implication of the putative negative regulation of bone

turnover by hematopoietic lineage cells would be that restoration of normal hematopoiesis following irradiation may be essential to restore normal bone turnover.

The major cause of death associated with acute exposure to high dose (6 Gy) gamma irradiation is infection. A radioconditioning dose of 0.5 mGy has been shown to reduce mortality in mice exposed to a challenging dose of γ-radiation [18]. The mechanism for the protective effect of prior exposure to the lower dose radiation is incompletely understood. However, more rapid recovery of hematopoietic cells, depressed tumor suppressor gene expression, and induction of antioxidative and repair enzymes appear to contribute to the protective effects [43-46]. Whatever the precise mechanisms for improved survival, a standard radioconditioning priming dose of 0.5 mGy was ineffective in moderating the acute skeletal effects of irradiation (6 Gy) on bone. Thus, a rapid restoration of bone marrow cell populations may be critical because relatively long duration studies failed to show skeletal recovery in mice exposed to high but sub-lethal doses of ionizing radiation [9, 10].

Bone marrow transplantation was effective in repopulating the bone marrow cavity following lethal irradiation. Megakaryocyte and total marrow cell density were normal two months following bone marrow transplantation. Additionally, adipocytes in the bone marrow were rare. These findings are significant because high dose radiation has been reported to deplete the megakaryocyte population and increase bone marrow adiposity [27, 47]. Also, GFP tracking studies demonstrate that the vast majority of hematopoietic cells and a lesser but substantial portion of the mesenchymal cells were derived from the donor mice. Importantly, bone marrow transplantation resulted in normalization of bone turnover. Although many of the bone architectural parameters did not differ between control and irradiated marrow transplanted mice, the transplanted mice had shorter tibia and site-specific reductions in fractional bone volume (lumbar vertebra but not distal femur metaphysis or epiphysis), connectivity density (lumbar vertebra and distal femur epiphysis but not distal femur metaphysis), and trabecular number (distal femur metaphysis but not lumbar vertebra or distal femur epiphysis). The failure of bone marrow transplantation to restore all bone values to normal is not surprising. Repopulation of the marrow with donor cells is time-dependent and donor cells would not directly contribute to enhancing recovery of growth plate cartilage. Also, high dose radiation followed by bone marrow transplantation during childhood impairs gonadal function in boys and girls [48]. Finally, the concomitant use of chemotherapy drugs which negatively and irreversibly impact bone mass and architecture may contribute to the detrimental skeletal effects of bone marrow transplantation in humans [49]. Consistent with a decrease in uterine weight observed in irradiated mice in the present study (data not shown), radiation has been shown to negatively impact the ovarian reserve and uterine growth and function and decrease serum estrogen levels [50-53]. Gonadal hormones, especially estrogen, are important regulators of bone metabolism [54]. Thus, radiation may either transiently or irreversibly affect the levels of gonadal hormones that influence bone metabolism [51]. In spite of these limitations, bone marrow transplantation in addition to preventing death, minimized development of skeletal abnormalities in lethally irradiated mice.

In summary, high dose whole-body γ-radiation results in a dramatic bone turnover response in which both formation and

resorption are increased. The increased turnover is temporally associated with bone marrow failure and may result from disturbed regulation of osteoblast and osteoclast differentiation by hematopoietic cells. Bone marrow transplantation, by restoring normal bone marrow function, is effective in restoring normal bone turnover following lethal irradiation.

Highlights.

- The radio-protective effects of low dose radiation and marrow transplantation on bone metabolism were evaluated.
- Marrow cell density decreased within 1 day of exposure to 6Gy.
- Osteoblast-lined bone perimeter and osteoclast-lined bone perimeter was increased following exposure to 6Gy.
- Prior exposure to low dose irradiation did not prevent the detrimental effects of high dose irradiation on bone.
- Bone marrow transplantation normalized marrow cell density, bone turnover, and most indices of bone architecture following irradiation.

Acknowledgements

This work was supported by NASA grant number NNX12AL24G (to RT Turner) and by National Institute of Health grant AR 060913 (to UT Iwaniec).

Footnotes

Disclosures: The authors have no conflict of interest.

Literature Cited

[1]. Mavrogenis AF, Pala E, Romantini M, Guerra G, Romagnoli C, Maccauro G, Ruggieri P. Side effects of radiation in musculoskeletal oncology: clinical evaluation of radiation-induced fractures. Int J Immunopathol Pharmacol. 2011;24:29–37. doi: 10.1177/03946320110241S207. [DOI] [PubMed] [Google Scholar]

[2]. Boehling NS, Grosshans DR, Allen PK, McAleer MF, Burton AW, Azeem S, Rhines LD, Chang EL. Vertebral compression fracture risk after stereotactic body radiotherapy for spinal metastases. J Neurosurg Spine. 2012;16:379–86. doi: 10.3171/2011.11.SPINE116. [DOI] [PubMed] [Google Scholar]

[3]. Williams HJ, Davies AM. The effect of X-rays on bone: a pictorial review. Eur Radiol. 2006;16:619–33. doi: 10.1007/s00330-005-0010-7. [DOI] [PubMed] [Google Scholar]

[4]. Mavrogenis AF, Papagelopoulos PJ, Romantini M, Guerra G, Ruggieri P. Side effects of radiation in musculoskeletal oncology. J Long Term Eff Med Implants. 2009;19:287–304. doi: 10.1615/jlongtermeffmedimplants.v19.i4.60. [DOI] [PubMed] [Google Scholar]

[5]. Dorr H, Meineke V. Acute radiation syndrome caused by accidental radiation exposure–therapeutic principles. BMC Med. 2011;9:126. doi: 10.1186/1741-7015-9-126. [DOI] [PMC free article] [PubMed] [Google Scholar]

[6]. Townsend LW. Implications of the space radiation environment for human exploration in deep space. Radiat Prot Dosimetry. 2005;115:44–50. doi: 10.1093/rpd/nci141. [DOI] [PubMed] [Google Scholar]

[7]. Prise KM, Saran A. Concise review: stem cell effects in radiation risk. Stem Cells. 2011;29:1315–21. doi: 10.1002/stem.690. [DOI] [PubMed] [Google Scholar]

[8]. Donnelly EH, Nemhauser JB, Smith JM, Kazzi ZN, Farfan EB, Chang AS, Naeem SF. Acute radiation syndrome: assessment and management. South Med J. 2010;103:541–6. doi: 10.1097/SMJ.0b013e3181ddd571. [DOI] [PubMed] [Google Scholar]

[9]. Bandstra ER, Pecaut MJ, Anderson ER, Willey JS, De Carlo F, Stock SR, Gridley DS, Nelson GA, Levine HG, Bateman TA. Long-term dose response of trabecular bone in mice to proton radiation. Radiat Res. 2008;169:607–14. doi: 10.1667/RR1310.1. [DOI] [PMC free article] [PubMed] [Google Scholar]

[10]. Green DE, Adler BJ, Chan ME, Rubin CT. Devastation of adult stem cell pools by irradiation precedes collapse of trabecular bone quality and quantity. J Bone Miner Res. 2012;27:749–59. doi: 10.1002/jbmr.1505. [DOI] [PubMed] [Google Scholar]

[11]. Willey JS, Livingston EW, Robbins ME, Bourland JD, Tirado-Lee L, Smith-Sielicki H, Bateman TA. Risedronate prevents early radiation-induced osteoporosis in mice at multiple skeletal locations. Bone. 2010;46:101–11. doi: 10.1016/j.bone.2009.09.002. [DOI] [PMC free article] [PubMed] [Google Scholar]

[12]. Joiner MC. Evidence for induced radioresistance from survival and other end points: an introduction.

Radiat Res. 1994;138:S5–8. [PubMed] [Google Scholar]

[13]. Smirnova OA, Yonezawa M. Radioprotection effect of low level preirradiation on mammals: modeling and experimental investigations. Health Phys. 2003;85:150–8. doi: 10.1097/00004032-200308000-00003. [DOI] [PubMed] [Google Scholar]

[14]. Heslet L, Bay C, Nepper-Christensen S. Acute radiation syndrome (ARS) – treatment of the reduced host defense. Int J Gen Med. 2012;5:105–15. doi: 10.2147/IJGM.S22177. [DOI] [PMC free article] [PubMed] [Google Scholar]

[15]. Herodin F, Mayol JF, Mourcin F, Drouet M. Which place for stem cell therapy in the treatment of acute radiation syndrome? Folia Histochem Cytobiol. 2005;43:223–7. [PubMed] [Google Scholar]

[16]. Lange C, Brunswig-Spickenheier B, Cappallo-Obermann H, Eggert K, Gehling UM, Rudolph C, Schlegelberger B, Cornils K, Zustin J, Spiess AN, Zander AR. Radiation rescue: mesenchymal stromal cells protect from lethal irradiation. PLoS One. 2011;6:e14486. doi: 10.1371/journal.pone.0014486. [DOI] [PMC free article] [PubMed] [Google Scholar]

[17]. Saha S, Bhanja P, Kabarriti R, Liu L, Alfieri AA, Guha C. Bone marrow stromal cell transplantation mitigates radiation-induced gastrointestinal syndrome in mice. PLoS One. 2011;6:e24072. doi: 10.1371/journal.pone.0024072. [DOI] [PMC free article] [PubMed] [Google Scholar]

[18]. Ito M, Shibamoto Y, Ayakawa S, Tomita N, Sugie C, Ogino H. Low-dose whole-body irradiation induced radioadaptive response in C57BL/6 mice. J Radiat Res (Tokyo) 2007;48:455–60. doi: 10.1269/jrr.07022. [DOI] [PubMed] [Google Scholar]

[19]. Herodin F, Bourin P, Mayol JF, Lataillade JJ, Drouet M. Short-term injection of antiapoptotic cytokine combinations soon after lethal gamma -irradiation promotes survival. Blood. 2003;101:2609–16. doi: 10.1182/blood-2002-06-1634. [DOI] [PubMed] [Google Scholar]

[20]. Iwaniec UT, Wronski TJ, Turner RT. Histological analysis of bone. Methods Mol Biol. 2008;447:325–41. doi: 10.1007/978-1-59745-242-7_21. [DOI] [PubMed] [Google Scholar]

[21]. DiCarlo AL, Poncz M, Cassatt DR, Shah JR, Czarniecki CW, Maidment BW. Medical countermeasures for platelet regeneration after radiation exposure. Report of a workshop and guided discussion sponsored by the National Institute of Allergy and Infectious Diseases, Bethesda, MD, March 22-23, 2010. Radiat Res. 2010;176:e0001–15. doi: 10.1667/rrol01.1. [DOI] [PMC free article] [PubMed] [Google Scholar]

[22]. Hui SK, Sharkey L, Kidder LS, Zhang Y, Fairchild G, Coghill K, Xian CJ, Yee D. The influence of therapeutic radiation on the patterns of bone marrow in ovary-intact and ovariectomized mice. PLoS One. 2012;7:e42668. doi: 10.1371/journal.pone.0042668. [DOI] [PMC free article] [PubMed] [Google

Scholar]

[23]. Wilcox R, Charlin V, Thompson K. New Monte Carlo results on the robstness of the ANOVA F, W, and F* statistics. Communication in Statistics: Simulation and Computation. 1986;15:933–944. [Google Scholar]

[24]. Lotinun S, Sibonga JD, Turner RT. Evidence that the cells responsible for marrow fibrosis in a rat model for hyperparathyroidism are preosteoblasts. Endocrinology. 2005;146:4074–81. doi: 10.1210/en.2005-0480. [DOI] [PubMed] [Google Scholar]

[25]. Dobnig H, Turner RT. Evidence that intermittent treatment with parathyroid hormone increases bone formation in adult rats by activation of bone lining cells. Endocrinology. 1995;136:3632–8. doi: 10.1210/endo.136.8.7628403. [DOI] [PubMed] [Google Scholar]

[26]. Power RA, Iwaniec UT, Magee KA, Mitova-Caneva NG, Wronski TJ. Basic fibroblast growth factor has rapid bone anabolic effects in ovariectomized rats. Osteoporos Int. 2004;15:716–23. doi: 10.1007/s00198-004-1595-4. [DOI] [PubMed] [Google Scholar]

[27]. Dominici M, Rasini V, Bussolari R, Chen X, Hofmann TJ, Spano C, Bernabei D, Veronesi E, Bertoni F, Paolucci P, Conte P, Horwitz EM. Restoration and reversible expansion of the osteoblastic hematopoietic stem cell niche after marrow radioablation. Blood. 2009;114:2333–43. doi: 10.1182/blood-2008-10-183459. [DOI] [PMC free article] [PubMed] [Google Scholar]

[28]. Erben RG. Bone-labeling techniques. In: An YH, Martin KL, editors. Handbook of Histology Methods for Bone and Cartilage. Humana Press; Totowa: 2003. pp. 99–117. [Google Scholar]

[29]. Bethel M, Srour EF, Kacena MA. Hematopoietic cell regulation of osteoblast proliferation and differentiation. Curr Osteoporos Rep. 2011;9:96–102. doi: 10.1007/s11914-011-0048-1. [DOI] [PMC free article] [PubMed] [Google Scholar]

[30]. Edwards JR, Mundy GR. Advances in osteoclast biology: old findings and new insights from mouse models. Nat Rev Rheumatol. 2011;7:235–43. doi: 10.1038/nrrheum.2011.23. [DOI] [PubMed] [Google Scholar]

[31]. Turner RT, Evans GL, Wakley GK. Reduced chondroclast differentiation results in increased cancellous bone volume in estrogen-treated growing rats. Endocrinology. 1994;134:461–6. doi: 10.1210/endo.134.1.7506213. [DOI] [PubMed] [Google Scholar]

[32]. Willey JS, Lloyd SA, Robbins ME, Bourland JD, Smith-Sielicki H, Bowman LC, Norrdin RW, Bateman TA. Early increase in osteoclast number in mice after whole-body irradiation with 2 Gy X rays. Radiat Res. 2008;170:388–92. doi: 10.1667/RR1388.1. [DOI] [PMC free article] [PubMed] [Google Scholar]

[33]. Bjarnason NH, Hassager C, Christiansen C. Postmenopausal bone remodelling and hormone replacement. Climacteric. 1998;1:72–9. doi: 10.3109/13697139809080684. [DOI] [PubMed] [Google Scholar]

[34]. Timins JK. Communication of benefits and risks of medical radiation: a historical perspective. Health Phys. 2011;101:562–5. doi: 10.1097/HP.0b013e3182259a71. [DOI] [PubMed] [Google Scholar]

[35]. Menagh PJ, Turner RT, Jump DB, Wong CP, Lowry MB, Yakar S, Rosen CJ, Iwaniec UT. Growth hormone regulates the balance between bone formation and bone marrow adiposity. J Bone Miner Res. 2010;25:757–68. doi: 10.1359/jbmr.091015. [DOI] [PMC free article] [PubMed] [Google Scholar]

[36]. Lowry MB, Lotinun S, Leontovich AA, Zhang M, Maran A, Shogren KL, Palama BK, Marley K, Iwaniec UT, Turner RT. Osteitis fibrosa is mediated by Platelet-Derived Growth Factor-A via a phosphoinositide 3-kinase-dependent signaling pathway in a rat model for chronic hyperparathyroidism. Endocrinology. 2008;149:5735–46. doi: 10.1210/en.2008-0134. [DOI] [PMC free article] [PubMed] [Google Scholar]

[37]. Shimizu T, Mehdi R, Yoshimura Y, Yoshikawa H, Nomura S, Miyazono K, Takaoka K. Sequential expression of bone morphogenetic protein, tumor necrosis factor, and their receptors in bone-forming reaction after mouse femoral marrow ablation. Bone. 1998;23:127–33. doi: 10.1016/s8756-3282(98)00086-6. [DOI] [PubMed] [Google Scholar]

[38]. Suva LJ, Seedor JG, Endo N, Quartuccio HA, Thompson DD, Bab I, Rodan GA. Pattern of gene expression following rat tibial marrow ablation. J Bone Miner Res. 1993;8:379–88. doi: 10.1002/jbmr.5650080315. [DOI] [PubMed] [Google Scholar]

[39]. Horowitz MC, Fretz JA, Lorenzo JA. How B cells influence bone biology in health and disease. Bone. 2010;47:472–9. doi: 10.1016/j.bone.2010.06.011. [DOI] [PMC free article] [PubMed] [Google Scholar]

[40]. Lorenzo J, Horowitz M, Choi Y. Osteoimmunology: interactions of the bone and immune system. Endocr Rev. 2008;29:403–40. doi: 10.1210/er.2007-0038. [DOI] [PMC free article] [PubMed] [Google Scholar]

[41]. Chen Z. The relationship between incidence of fractures and anemia in older multiethnic women. J Am Geriatr Soc. 2010;58:2337–44. doi: 10.1111/j.1532-5415.2010.03183.x. [DOI] [PMC free article] [PubMed] [Google Scholar]

[42]. Haidar R, Musallam KM, Taher AT. Bone disease and skeletal complications in patients with beta thalassemia major. Bone. 2011;48:425–32. doi: 10.1016/j.bone.2010.10.173. [DOI] [PubMed] [Google Scholar]

[43]. Saini D, Shelke S, Mani Vannan A, Toprani S, Jain V, Das B, Seshadri M. Transcription profile of DNA damage response genes at G(0) lymphocytes exposed to gamma radiation. Mol Cell Biochem. 2012;364:271–81. doi: 10.1007/s11010-012-1227-9. [DOI] [PubMed] [Google Scholar]

[44]. Szumiel I. Adaptive response: stimulated DNA repair or decreased damage fixation? Int J Radiat Biol. 2005;81:233–41. doi: 10.1080/09553000500077047. [DOI] [PubMed] [Google Scholar]

[45]. Vares G, Wang B, Tanaka K, Shang Y, Fujita K, Hayata I, Nenoi M. Trp53 activity is repressed in radio-adapted cultured murine limb bud cells. J Radiat Res (Tokyo) 2011;52:727–34. doi: 10.1269/jrr.10092. [DOI] [PubMed] [Google Scholar]

[46]. Wharton W. Repression of G0/G1 traverse in human fibroblasts exposed to low levels of ionizing radiation. J Biol Chem. 2004;279:43667–74. doi: 10.1074/jbc.M407959200. [DOI] [PubMed] [Google Scholar]

[47]. Mitchell MJ, Logan PM. Radiation-induced changes in bone. Radiographics. 1998;18:1125–36. doi: 10.1148/radiographics.18.5.9747611. quiz 1242-3. [DOI] [PubMed] [Google Scholar]

[48]. Mayer EI, Dopfer RE, Klingebiel T, Scheel-Walter H, Ranke MB, Niethammer D. Longitudinal gonadal function after bone marrow transplantation for acute lymphoblastic leukemia during childhood. Pediatr Transplant. 1999;3:38–44. doi: 10.1034/j.1399-3046.1999.00006.x. [DOI] [PubMed] [Google Scholar]

[49]. Hayward R, Iwaniec UT, Turner RT, Lien CY, Jensen BT, Hydock DS, Schneider CM. Voluntary wheel running in growing rats does not protect against doxorubicin-induced osteopenia. J Pediatr Hematol Oncol. 2013;35:e144–8. doi: 10.1097/MPH.0b013e318279b1fb. [DOI] [PubMed] [Google Scholar]

[50]. Critchley HO, Wallace WH. Impact of cancer treatment on uterine function. J Natl Cancer Inst Monogr. 2005:64–8. doi: 10.1093/jncimonographs/lgi022. [DOI] [PubMed] [Google Scholar]

[51]. Gracia CR, Sammel MD, Freeman E, Prewitt M, Carlson C, Ray A, Vance A, Ginsberg JP. Impact of cancer therapies on ovarian reserve. Fertil Steril. 2012;97:134–40 e1. doi: 10.1016/j.fertnstert.2011.10.040. [DOI] [PMC free article] [PubMed] [Google Scholar]

[52]. Inskip PD, Eby NL, Cookfair D, Freedman RS, Richardson GS, Wactawski-Wende J, Hoover RN, Boice JD., Jr. Serum estrogen and androgen levels following treatment for cervical cancer. Cancer Epidemiol Biomarkers Prev. 1994;3:37–45. [PubMed] [Google Scholar]

[53]. Larsen E. Radiotherapy at a young age reduces uterine volume of childhood cancer survivors. Acta Obstet Gynecol Scand. 2004;83:96–102. doi: 10.1111/j.1600-0412.2004.00332.x. [DOI] [PubMed] [Google Scholar]

[54]. Turner RT, Riggs BL, Spelsberg TC. Skeletal effects of estrogen. Endocr Rev. 1994;15:275–300. doi:

10.1210/edrv-15-3-275. [DOI] [PubMed] [Google Scholar]